

Porosity Determination by Using Stochastics Method

UDK 681.586:532.696
 IFAC IA 4.2.2

Original scientific paper

In response to a need for a more accurate porosity measuring method for small solid samples (approximately 1 g in mass) the porosity measurement sensor using the sensitive capacitive-dependent crystal was developed. This paper presents the new sensor and the probe sensitivity (dependence of df on the volume). In addition, the new idea of excitation of the entire sensor with stochastic test signals is described, and the porosity measuring method is provided. The latter includes the influence of test signals on the weighting function uncertainty. The experimental results of the porosity determination in volcanic rock samples are presented. The uncertainty of the porosity measurement is less than 0.1 % (Temp=10-30 °C).

Key words: porosity, volcanic rock, capacitive-dependent crystal, stochastics method

1 INTRODUCTION

Porosity is defined as the ratio of the volume of voids to the total volume of the material.

Porosity in rocks originates as *primary porosity* during sedimentation or organogenesis and as *secondary porosity* at later stages of the geological development. In sedimentary rocks the porosity is further classified as intergranular porosity between grains, intragranular or intercrystalline porosity within grains, fracture porosity caused by mechanical or chemical processes, and cavernous porosity caused by organisms or chemical processes [1].

Solid rock is often not so solid. Sandstone might have started out as a sand dune or a beach, which got buried and compressed. But spaces remain between the particles. These spaces, or pores, are where oil and gas may be found. If you look at a sponge you can see many open spaces. Sandstone is like that, only the spaces are generally much smaller, so small that they cannot be seen without a microscope [2, 3].

Soils, too, contain pores, which can be classified as micro and macro. Pore diameters larger than 0.06 mm are called macropores and those less as micropores [2-5]. Soils are a heterogeneous composition of substances such as rock grains, water, air and other admixtures. Rock grains are of different sizes, shapes and mineralogical composition. They are bound into a more or less dense structure. Among these grains we can always find voids, which indicates that soils can be justly considered a porous ma-

terial. These voids are filled with air or water, or with air and water. In the first case the soil is referred to as dry, in the second case it is saturated and in the third case it is naturally humid. It is well known that the properties of soils considerably depend on the distribution of pores in the structure, their size, the percentage of pore volumes in relation to the total volume, the quantity of water inside them, etc. Thus the number and size of pores directly relate to soil organic matter content, texture and structure. Texture refers to the relative proportions of sand, silt and clay, while structure is the arrangement of soil particles into aggregates [1, 6-8].

Soils may be considered as a porous three phase system composed of air, water and solids. In this three-phase soil system, the density ρ of soils is defined as the ratio of the sum of mass m to the sum of volume V of various soil phases [9-12].

$$\rho = \frac{\sum_i m_i}{\sum_i V_i}, \quad (1)$$

$$\sum_i m_i = m_s + m_w + m_a + m_{ad}, \quad (2)$$

where

- s solid phase
- w water phase
- a air phase
- ad admixture.

$$\sum_i V_i = V_s + V_w + V_a + V_{ad}, \quad (3)$$

$$\rho = \frac{m_s + m_w + m_a + m_{ad}}{V_s + V_w + V_a + V_{ad}}. \quad (4)$$

Equation (4) can also be rewritten as

$$\rho = \frac{\rho_s V_s + \rho_w V_w + \rho_a V_a + \rho_{ad} V_{ad}}{V_s + V_w + V_a + V_{ad}}, \quad (5)$$

where solid particle density is

$$\rho_s = \frac{W_s}{V_s}, \quad (6)$$

water phase density is

$$\rho_w = \frac{W_w}{V_w}, \quad (7)$$

air phase density is

$$\rho_a = \frac{W_a}{V_a}, \quad (8)$$

and soil admixture density is

$$\rho_{ad} = \frac{W_{ad}}{V_{ad}}, \quad (9)$$

with weight W_i and volume V_i of various phases. Instead of density, the specific gravity can be written. From equation (5) we can write

$$\gamma = \frac{(\rho_s V_s + \rho_w V_w + \rho_a V_a + \rho_{ad} V_{ad}) \cdot g}{V_s + V_w + V_a + V_{ad}}. \quad (10)$$

In practice, we can define mass as the ratio of weight of soil to gravity

$$m = \frac{W}{g}. \quad (11)$$

During weighting in air the mass must be reduced due to the presence of the air

$$m_s = \frac{W_s}{g} + \rho_a \cdot V_s, \quad (12)$$

$$m_w = \frac{W_w}{g} + \rho_a \cdot V_w, \quad (13)$$

$$m_{ad} = \frac{W_{ad}}{g} + \rho_a \cdot V_{ad}. \quad (14)$$

Porosity of soil is defined by two parameters – void ratio e and porosity parameter η . The void ratio e is defined as the ratio of volume of pores to volume of particles

$$e = \frac{V_w + V_a}{V_s}, \quad (15)$$

$$e_w = \frac{V_w}{V}, \quad (16)$$

$$e_a = \frac{V_a}{V}. \quad (17)$$

The porosity parameter η is defined as the ratio of volume of pores to volume of soil samples

$$\eta = \frac{V_w + V_a}{V} = \frac{V_w + V_a}{V_s + V_w + V_a}, \quad (18)$$

$$\eta_w = \frac{V_w}{V} = \frac{V_w}{V_s + V_w + V_a}, \quad (19)$$

$$\eta_a = \frac{V_a}{V} = \frac{V_a}{V_s + V_w + V_a}. \quad (20)$$

The water content w is defined as the ratio of the weight of water to the weight of soil particles

$$w = \frac{W_w}{W_s} = \frac{W - W_a - W_s}{W_s}. \quad (21)$$

The absolute water content w_a is defined as the ratio of the weight of water to the weight of soil samples

$$w_a = \frac{W_w}{W} = \frac{W - W_a - W_s}{W}. \quad (22)$$

The degree of saturation S_r is defined as the ratio of the volume of pores saturated with water to the volume of all pores

$$S_r = \frac{V_w}{V_w + V_a} = \frac{\eta_w}{\eta_w + \eta_a}. \quad (23)$$

1.1 Porosity determination methods

There are many different porosity measurement methods. The simplest one is the determination of porosity by saturation method (Figure 1) [1, 2]. In this method, the beakers are first filled to the same mark with gravel, sand, silt or mixture of these three materials. Then the water is poured into each of the beakers until it reaches the top of each material.

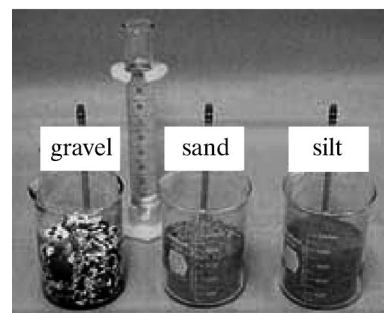


Fig. 1 Determination of porosity by saturation

Porosity is determined by dividing the volume of water that you were able to pour into the material by the total volume of that material. The result is expressed as a percentage. It dictates how much water a saturated material can contain and has an important influence on bulk properties of material, e.g. bulk density, heat capacity, seismic velocity, etc.

$$\eta = \frac{V_{\text{void}}}{V_{\text{total}}} \cdot 100 \% \quad (24)$$

where

$$\begin{aligned} V_{\text{void}} &- \text{pore space volume} \\ V_{\text{total}} &- \text{total volume.} \end{aligned}$$

The imaging porosity method aims to identify and quantify different pore systems to determine the nature and abundance of matrix and macroporosity. Matrix porosity is characterised from digital images obtained from thin sections cut from core plugs. Microporosity is qualified with back-scatter SEM or by 25x microscope objective; larger matrix pores are quantified with 10x or 4x microscope objectives. In each digital image the porosity is »segmented« by the image analysis software and a second image is created in which the porosity is picked out in false colour [13–15].

The helium pycnometer method uses helium, which as a very small atom penetrates all the cracks and holes in the rock, and all the boundaries between mineral grains, but does not get inside the grains. The pycnometer consists of two chambers, connected by a tube with a valve in it. Each chamber has assorted sensors to measure temperature and pressure, which are read out to a computer. The idea is to measure the pressure difference between the two containers, one of which has the sample material in it. The volumes of the two chambers are known very precisely, and the difference in volumes available to the gas is due to the presence of the sample in one of the chambers. The difference in the volume of open space between the two chambers is related to the difference in the pressures. The porosity of the sample is the percentage difference between the grain volume and bulk volume, divided by the bulk volume [16].

Porosity can also be determined by other conventional methods such as adsorption method, mercury porosimetry, capillary method, dielectric method, analytical method, proton nuclear magnetic resonance, chromatography and ultrasound method [17, 18].

The new porosity measuring method described in this paper uses a highly sensitive sensor with improved uncertainty of measuring results and reduced influence of disturbing noise signals [19]. In comparison to the helium pycnometer method it is

a lot simpler. In addition, the water is not poured on the material. Instead, the soil or rock sample is immersed in the water.

Most capacitive bridge methods can be adapted to three-terminal measurements by the addition of components to balance the ground admittances [20–22]. However, the balance conditions for these and the main bridge being interdependent, the balancing process can become very tedious. Also, the ratio signal/noise is supposed to be high.

The well-known method is Miller's etalon [23] which is designed to sense small changes in the $\cong 4$ pF capacitor from the phase change of a series-resonant circuit. The weakness of Miller's etalon is a greater sensitivity to phase noise than with the bridge method, which is due to higher frequencies (up to 45 MHz).

An alternative approach has been described by Van Degriift [24] who used very sensitive tunnel-diode oscillator systems for measuring extremely small capacitance changes. This gain in sensitivity is somewhat offset by a loss in stability.

2 THE POROSITY SENSOR

The porosity sensor uses sensitive capacitive-dependent crystals (40 MHz with stability of ± 1 ppm in the temperature range from -5 to $+55$ °C) due to stability and the long-term repetition (Figure 2).

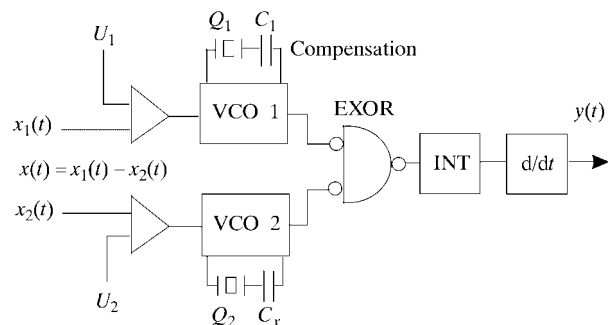


Fig. 2 Sensor structure

Two pseudo stochastic three-state signals $x_1(t)$ and $x_2(t)$ are used to influence the frequencies of the two quartz oscillators [25–27]. The frequency of oscillator 1 is 40 MHz and that of oscillator 2 is 40.001 MHz [28, 29]. The output of the pulse-width modulator (EXOR) is a pulse-width signal which is compensated for temperature and voltage drift.

The sensor probe C_x is a capacitor on the outer surface of the glass test tube (Figure 3) [30]. The crystal is used as a stable oscillation element whose substitutional electrical structure only is being chan-

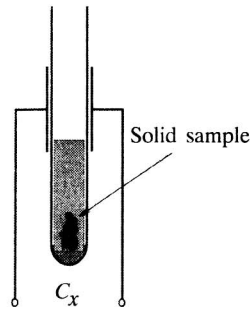


Fig. 3 Glass test tube

ged through the variation of the series capacitance C_x . The values in the quartz substitutional electrical structure and the capacitance $C_x = 5$ pF are measured with impedance/gain phase analyser HP 4194A [29].

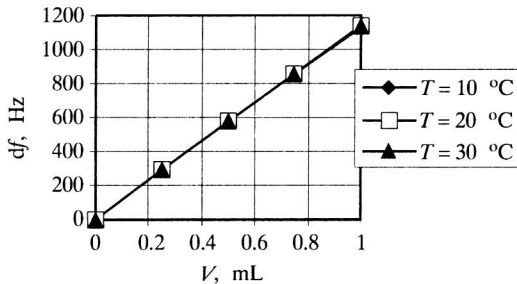


Fig. 4 The probe dependence df on the volume with signals $x_1(t)$ and $x_2(t)$

The change of the liquid level causes the change of capacitance and frequency change in oscillator 2 (Figure 2, Figure 3). The probe dependence df on the volume is shown in Figure 4. The frequency measurement uncertainty is ± 0.1 Hz. The results suggest that the change in frequency is proportional to the volume in the range 0–1 mL.

3 REDUCTION OF THE MEASUREMENT UNCERTAINTY

The uncertainty of the measuring results is improved by the direct digital method (DDM), which reduces the influence of disturbances [19]

$$\Phi_{xy}(\tau) = \sum_{u=0}^{t_{meas}} g(u) \cdot \Phi_{xx}(\tau-u). \quad (25)$$

For every value of τ , one equation with various numbers of elements is obtained. To calculate the value of the weighting functions $g(0), g(1), \dots, g(L)$, the equations are united in the system with $L+1$ equations as (26)

$$\begin{bmatrix} \Phi_{xy}(-P+L) \\ \vdots \\ \Phi_{xy}(-1) \\ \Phi_{xy}(0) \\ \Phi_{xy}(+1) \\ \vdots \\ \Phi_{xy}(M) \end{bmatrix} = \begin{bmatrix} \Phi_{xx}(-P+L) & \dots & \Phi_{xx}(-P) \\ \vdots & \dots & \vdots \\ \Phi_{xx}(-1) & \dots & \Phi_{xx}(-1-L) \\ \Phi_{xx}(0) & & \Phi_{xx}(-L) \\ \Phi_{xx}(+1) & & \Phi_{xx}(1-L) \\ \vdots & \dots & \vdots \\ \Phi_{xx}(M) & & \Phi_{xx}(M-L) \end{bmatrix} \begin{bmatrix} g(0) \\ \vdots \\ \vdots \\ \vdots \\ \vdots \\ \vdots \\ g(L) \end{bmatrix}$$

$$\hat{\Phi}_{xy} = \hat{\Phi}_{xx} \cdot g. \quad (26)$$

The biggest negative time move $\tau_{min} = -P$ and the biggest positive one $\tau_{max} = M$ were used. The system of equations has thus $P-L+M+1$ number of equations. If $M = -P+2L$ is chosen, $L+1$ number of equations remain, so that $\hat{\Phi}_{xx}$ becomes a square matrix and we get

$$\hat{g} = \hat{\Phi}_{xx}^{-1} \cdot \hat{\Phi}_{xy}. \quad (27)$$

If $P=L$ is determined, then the same number of values (symmetrical auto-correlation functions (AKF) because $\tau_{min} = -P = -L$ and $\tau_{max} = M = L$ for the positive and negative τ is used to calculate AKF $\Phi_{xx}(\tau)$. The calculation of the weighting function is simplified if the input signal is white noise with the auto-correlation function as

$$\Phi_{xx}(\tau) = \sigma_x^2 \cdot \delta(\tau) = \Phi_{xx}(0) \cdot \delta(\tau) \quad (28)$$

$$\delta(\tau) = \begin{cases} 1 & \text{for } \tau = 0 \\ 0 & \text{for } |\tau| \neq 0 \end{cases}. \quad (29)$$

It follows that

$$\hat{g}(\tau) = \frac{1}{\hat{\Phi}_{xx}(0)} \cdot \hat{\Phi}_{xy}(\tau). \quad (30)$$

Having formulated (27) and having considered the measurement time t_{meas} , we get the weighting function $\hat{g}(\tau)$ (30) [19].

4 POROSITY MEASUREMENT

Due to the specially chosen test signals $x_1(t)$ and $x_2(t)$ the function $\Phi_{xy1}(\tau)$ begins in the origin of coordinates and ends on the X axis when $\tau = t_{meas}$ (Figure 5).

Consequently, the porosity is defined as a change of area (surface) between the functions $\Phi_{xy2}(\tau)$ and $\Phi_{xy1}(\tau)$, whose change is defined by capacitance C_x . In this way the test signal has been considered throughout the entire t_{meas} period, as well as the

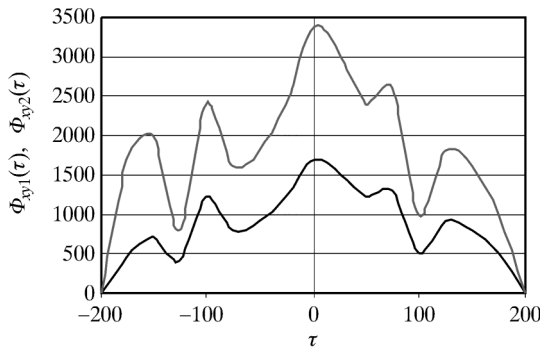


Fig. 5 Functions $\Phi_{xy1}(\tau)$ and $\Phi_{xy2}(\tau)$

sign change compensation in the calculation of the cross-correlation function. Comparing to the measurements that are not DDM method based the improvement of the ratio signal/noise by $\cong 30$ dB is the most significant gain.

4.1 The analysis of physical soil properties

Measurements are conducted according to standard procedures. A three-stage measurement for the determination of physical properties is suggested.

4.1.1 Stage I

As in conventional measurements the weight of a representative soil sample T is given. The sample is dried and dry weight is given T_s . The weight of water T_w is obtained from the difference of the two weights

$$T_w = T - T_s. \quad (31)$$

The natural humidity w of the soil is calculated

$$w = \frac{T_w}{T_s}. \quad (32)$$

The share of grain weight ν_s and the share of water weight ν_w in relation to the total sample weight are calculated

$$\nu_s = \frac{T_s}{T}, \quad (33)$$

$$\nu_w = \frac{T_w}{T}. \quad (34)$$

All the remaining characteristics determined in conventional tests are given in the first stage.

4.1.2 Stage II

The second stage is performed on a random number of small samples. Each sample must be dry and in bulk. All samples are weighted T_{si} . Each sample is put into a glass tube and its volume V_{si} is measured. The measurement is performed until the fi-

nal state towards which the measurement limits is reliably predicted. The specific gravity of the si -th soil sample is calculated

$$\gamma_{si} = \frac{T_s}{V_s}. \quad (35)$$

4.1.3 Stage III

The third stage is performed on a random number of small naturally humid and undeformed soil samples, with natural form and dimension. All natural humid samples are weighted T_s . Each sample is put into a glass tube and its volume is measured V_s . The measurement is performed until the final state towards which the measurement limits is reliably predicted. From measuring and equation (35) weight of water is calculated

$$T_s = \nu_s \cdot T. \quad (36)$$

The specific gravity of the i -th soil sample is calculated.

$$T = T_s + T_w. \quad (37)$$

The sample is immersed into the glass tube and the total volume V and the volume of air V_a in the sample are measured. The volume of water in the sample is measured from the known water weight and (measured) temperature

$$V_w = \frac{T_w}{\gamma_w}, \quad (38)$$

$$\gamma_w = f(\text{temp}), \quad (39)$$

$$V_s = V - V_a - V_w. \quad (40)$$

The density (volume weight) is determined

$$\gamma = \frac{T}{V}, \quad (41)$$

$$\rho = \frac{T}{V \cdot g}. \quad (42)$$

The porosity of the soil is determined

$$e = \frac{V_w + V_a}{V}, \quad (43)$$

$$e_w = \frac{V_w}{V}, \quad (44)$$

$$e_a = \frac{V_a}{V}, \quad (45)$$

$$\eta = \frac{V_w + V_a}{V}, \quad (46)$$

$$\eta_w = \frac{V_w}{V}, \quad (47)$$

$$\eta_a = \frac{V_a}{V}. \quad (48)$$

The degree of the soil saturation S_r is determined

$$S_r = \frac{V_w}{V_s + V_w}. \quad (49)$$

4.2 The small volume measurement technique

Glass tubes filled with fluid are used for measurements. For each test, the fluid level in the glass tube is measured and the changes of the volume in the glass tube are measured indirectly from the changed fluid levels. The mechanical nonlinearities of the glass tube which, according to the producer's data do not exceed 0.01 %, are taken into account.

4.3 Calibration

The frequency is simultaneously converted into volume units by calibrating the ratio between the frequency and the volume for each glass tube. Mercury, whose mass is measured at an error of 0.01 % (at known temperature) is used for calibration [31]. The dependence can be linearized by using the spline method.

4.4 The influence of temperature and measurement error

The influence of temperature on measurements is considered in three ways. We must know the influence of the temperature on the measuring equipment, on the measuring medium in which the measurement is performed (i.e. the fluid in which the test is carried out), and the influence of the soil's temperature on its physical properties [31].

The temperature of the environment affects the linearity of the measuring sensor. Calibration is used to establish the measurement error of the sensor which is 0.03 %. If the relation between the output frequency and the volume is known (Figure 4), we get

$$V(\text{Temp}) = V(\text{Temp}_0) + \Delta V(\text{Temp}). \quad (50)$$

Equation (52) gives the correction of the measurement with respect to temperature changes. Temperature changes also affect the volume of the measuring medium, i.e. of the soil sample. Consequently, the change of volume due to temperature changes is expressed in the determination of the soil's specific gravity as follows

$$\gamma(\text{Temp}) = \gamma(\text{Temp}_0) + \Delta\gamma(\text{Temp}). \quad (51)$$

In conditions of linear temperature relationship inside a certain temperature range it holds true that

$$V(\text{Temp}) = V_s(\text{Temp}_0) \cdot (1 + \alpha_{V_s}(\text{Temp} - \text{Temp}_0)). \quad (52)$$

The change of volume due to temperature changes in naturally humid soils is expressed as the sum of volume changes of all soil phases

$$dV(\text{Temp}) = dV_s(\text{Temp}) + dV_w(\text{Temp}) + dVa(\text{Temp}). \quad (53)$$

The total measurement error of the porosity sensor in relation to individual partial influences such as glass tube nonlinearity, calibration with mercury, the influence of temperature on the sensor (Figure 4), linearization of df on V , frequency measurement $y(t)$ (Figure 2), specific soil weight (51), change of water volume in the test tube and the change of sample volume $dV(\text{Temp})$ (53) is 0.1 %.

5 EXPERIMENTAL POROSITY MEASUREMENT

To test the new method, volcanic rock samples, which are known for their porosity, were selected for experimental determination of porosity (Figure 6).

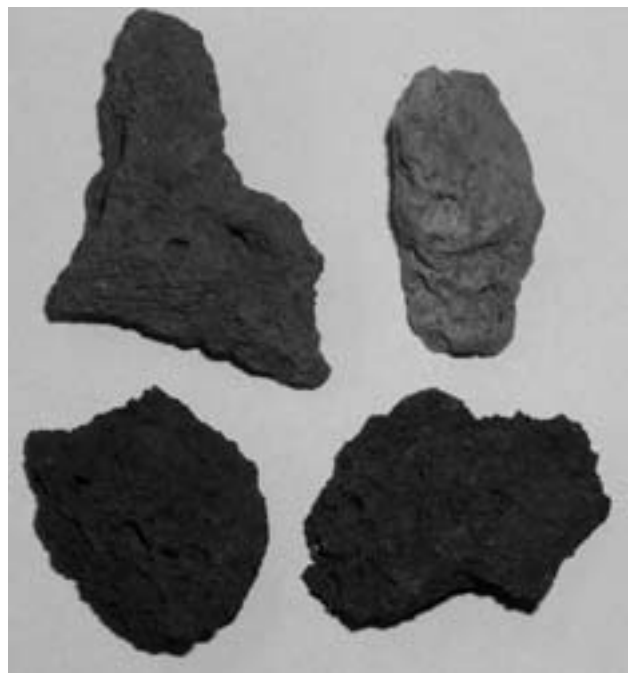


Fig. 6 Four characteristic porous volcanic rock samples of 1 mL in size and 1 g in mass (see page 210)

All test samples were randomly selected. To determine the porosity of a random solid sample (at 20 °C), the latter is immersed in water contained in a test tube around which the capacitor C_x is placed (Figure 3). The volume of the sample is measured. In the first case, the glass solid sample with 0 % porosity was immersed (Figure 7).

The frequency did not change, which indicates that there was no air leak. In the second case, a dry

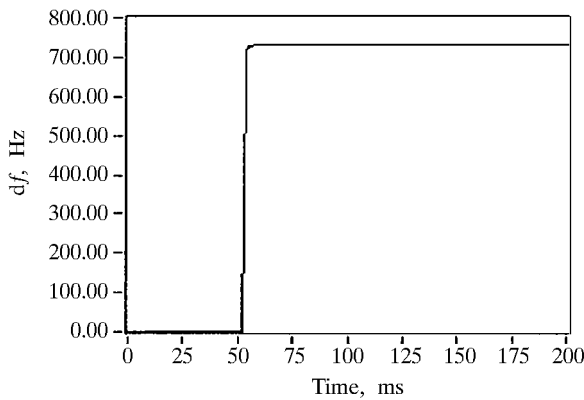


Fig. 7 Measurement of sample having 0 % porosity

randomly selected volcanic rock sample (weighting 0.821 g) was immersed in the water. Since the sample was porous, the air leaked, which was reflected in the dynamic change of frequency (Figure 8) [32].

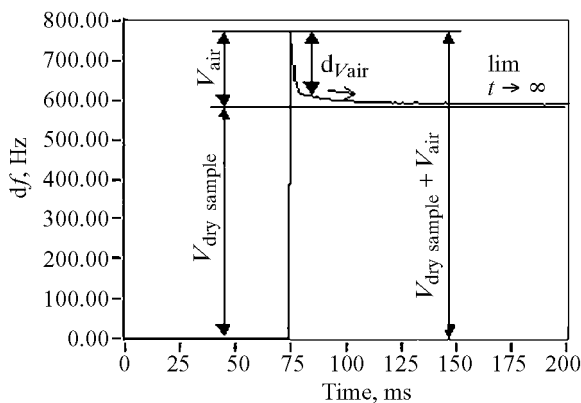


Fig. 8 Air leak after sample immersion

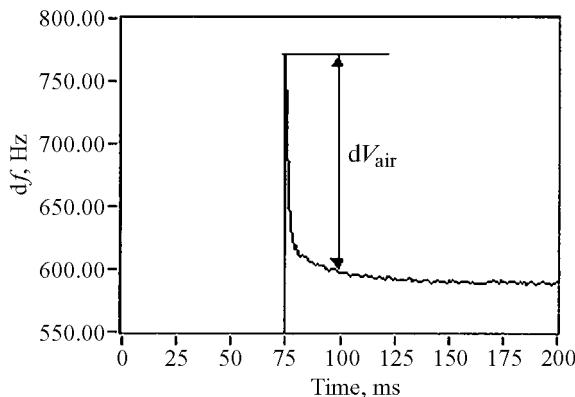


Fig. 9 Air leak after sample immersion (enlarged Figure 8)

The measurement is performed until the final state towards which the measurement limits is reliably predicted. Depending on the degree of porosi-

ty, this saturation limit is higher or lower (Figure 8). A more clear image of the air leak and the volume change within 200 ms time span is given on Figure 9 (enlarged Figure 8).

At known temperature the sample porosity can be determined

$$\eta = \frac{V_{\text{air}}}{V_{\text{dry sample}} + V_{\text{air}}} \quad (54)$$

The sample porosity on Figure 8 was 23.81 %.

6 CONCLUSION

The porosity sensor using the capacitive-dependent crystals has been described and the dependence of df on the volume of the sensor probe has been presented. In addition, the porosity measurement using the surface-measuring method has been given. The latter includes the influence of test signals on the weighting function uncertainty.

The formation of the cross-correlation function between the test signal $x(t)$ and the system response $y(t)$ decreases the influence of all disturbing signals that are not correlated to the test signal $x(t)$ for ≈ 30 dB [19]. Other advantages of the proposed method are high sensitivity, high stability, a series resonant circuit which is not composed of the elements L and C , the ratio signal/noise does not affect the accuracy of measurements, reduced disturbances due to the structure and the method, the long-term repetition, reduced hysteresis [28] and low cost. It should be noted, however, that pairs of crystals with similar temperature characteristics should be used. The accuracy and repeatability are determined only with the temperature frequency difference of the crystal pairs [33].

Experimental results confirm the applicability of the porosity sensor. The equipment enables very accurate measurements. The subsequent computer analysis and statistical processing of obtained results additionally reduce the measurement error. In addition to high quality interpretation of results, this method also offers their immediate on-site interpretation, if the specific gravity is known. Furthermore, the measurements can be performed on a large number of small samples of any shape which allows the establishment of the local heterogeneity of the material. The sample size can be adjusted to the granulometric composition of soils.

REFERENCES

- [1] J. Schoper, **Porosität und Permeabilität**. Physikalische Eigenschaften der Gesteine, vol. V/Ia, s. 184, 1982.
- [2] A. Netto, **Pore-size Distribution in Sandstones**. Bull. Appl. Math., vol. 77, pp. 1101, 1993.

- [3] P. Sheng, **Effective Medium Theory of Sedimentary Rocks**. Phys. Rev. B., vol. 41, pp. 4507, 1993.
- [4] J. Howard, W. Kenyon, **Determination of Pore Size Distribution in Sedimentary Rocks by Proton Nuclear Magnetic Resonance**. Marine and Petroleum Geology, vol. 9, pp. 139, 1992.
- [5] S. Sakai, **Determination of Pore Size and Pore Size Distribution**. Journal of Membrane Science, vol. 96, pp. 91, 1994.
- [6] C. Jacquin, P. Adler, **Fractal Porous Media II: Geometry of Porous Geological Structures**. Transport in Porous Media, vol. 2, pp. 28, 1987.
- [7] P. Doyen, **Permeability, Conductivity and Pore Geometry of Sandstone**. J. Geophys. Res., vol. 93, pp. 7729, 1988.
- [8] J. Harlan, D. Picot, P. Loll, **Calibration of Size-exclusion Chromatography: Use of a Double Gaussian Distribution Function to Describe Pore Sizes**. Analytical Biochemistry, vol. 224, pp. 577, 1995.
- [9] M. Spearing, P. Matthews, **Modelling Characteristic Properties of Sandstones**. Transport in Porous Media, vol. 6, pp. 71, 1991.
- [10] G. Matthews, M. Spearing, **Measurement and Modelling of Diffusion, Porosity and Other Pore Level Characteristics of Sandstones**. Marine and Petroleum Geology, vol. 9, pp. 146, 1992.
- [11] M. Kwiecen, I. MacDonald, F. Dullien, **Three-dimensional Reconstruction of Porous Media from Serial Section Data**. J. Microsc., vol. 159, pp. 343, 1990.
- [12] K. Meyer, P. Lorenz, B. Böhl-Kuhn, P. Klobes, **Porous Solids and their Characterization**. Cryst. Res. Techn., vol. 29, pp. 903, 1994.
- [13] J. Berryman, **Measurement of Spatial Correlation Functions Using Image Processing Techniques**. J. Appl. Phys., vol. 57, pp. 2374, 1985.
- [14] W. W. Chen, B. Dunn, **Characterization of Pore Size Distribution by Infrared Scattering**. Journal of the American Ceramic Society, vol. 76, pp. 2086, 1993.
- [15] J. Fredrich, B. Menendez, T. Wong, **Imaging the Pore Structure of Geomaterials**. Science, vol. 268, pp. 276, 1995.
- [16] H. Franz, **Herstellung von Drucksensoren**. Feinwerktechnik & Meßtechnik 95, H. 3, s. 145–151, 1987.
- [17] J. Fripiat, **Porosity and Adsorption Isotherms**. Fractal Approach to Heterogeneous Chemistry, Wiley, pp. 28, 1989.
- [18] G. P. P. Gunarathne, K. Christidis, **Measurements of Surface Texture Using Ultrasound**. IEEE Trans. Instrum. Meas., 50 (5), October, pp. 1144–1148, 2002.
- [19] K. W. Bonfig, **Das Direkte Digitale Messverfahren (DDM) als Grundlage einfacher und dennoch genauer und stör-sicherer Sensoren**. Sensor nov., s. 223–228, 1988.
- [20] M. C. McGregor, J. F. Hersh, R. D. Cutkosky, F. K. Harris, F. R. Kotter, **New Apparatus at the National Bureau of Standards for Absolute Capacitance Measurement**. IRE Trans. Instr. 1–7 (3–4), pp. 253–61, 1958.
- [21] A. M. Thompson, **The Precise Measurement of Small Capacitances**. IRE Trans. Instr. 1–7(3–4), pp. 245–53, 1958.
- [22] C. Moon, C. M. Sparks, **Standards for Low Values of Direct Capacitance**. J. Res. NBS, vol. 41, Nov., pp. 497–507, 1948.
- [23] G. L. Miller, E. R. Wagner, **Resonant Phase Shift Technique for the Measurement of Small Changes in Grounded Capacitors**. Rev. Sci. Instrum. 61(4), pp. 1267, 1990.
- [24] C. T. Van Degrieff, **Modeling of Tunnel Diode Oscillators**. Rev. Sci. Instrum. 52(5), May, pp. 712–723, 1981.
- [25] E. Bartels, T. Funk, **Correlation Method for Determination of the Time Constants of Impedances Applied to Electrical Model Networks and to a Liquid Capacitor**. J. Phys. E. 16, pp. 1105, 1983.
- [26] K. Dmowski, **A New Correlation Method for Improvement in Selectivity of Bulk Trap Measurements from Capacitance and Voltage Transients**. Rev. Sci. Instrum. 61(4), April, pp. 1319–1325, 1990.
- [27] M. Bertocco, A. Flammini, D. Marioli, A. Taroni, **Fast and Robust Estimation of Resonant Sensors Signal Frequency**. IEEE Trans. Instrum. Meas., 51 (2), April, pp. 326–330, 2002.
- [28] V. Matko, J. Koprivnikar, **Capacitive Sensor for Water Absorption Measurement in Glass-fiber Resins Using Quartz Crystals**. IAAMSA: South African branch of the Academy of Nonlinear Sciences, Proceedings, Durban, South Africa, pp. 440–443, 1998.
- [29] V. Matko, J. Koprivnikar, **Quartz Sensor for Water Absorption Measurement in Glass-fiber Resins**. IEEE Trans. Instrum. Meas., 47 (5), Oct., pp. 1159–1162, 1998.
- [30] M. Stucchi, K. Maex, **Frequency Dependence in Interline Capacitance Measurements**. IEEE Trans. Instrum. Meas., 51 (3), Jun., pp. 537–543, 2002.
- [31] R. C. Weast, **CRC Handbook of Chemistry and Physics**. 67th edition, Boca Raton, Florida, pp. E49–E52, 1987.
- [32] P. Gennes, **Wetting: Statics and Dynamics**. Rev. Mod. Phys., vol. 57, pp. 827, 1985.
- [33] J. Fraden, **Modern Sensors**. American Institute of Physics, ISBN 1-56396-538-0, 1997.

Određivanje poroznosti primjenom stohastičke metode. Razvijena je metoda za mjerenje poroznosti malih čvrstih uzoraka tla (približne mase od 1 g) s pomoću kapacitivno osjetljivog kristala. U radu su opisani novorazvijeni senzor i osjetljivost probe (ovisnost promjene frekvencije o volumenu). U nastavku je prikazana nova ideja pobude cijelog senzora stohastičkim ispitnim signalima kao nova metoda mjerenja poroznosti. Ona uključuje utjecaj ispitnog signala na težinsku funkciju mjerne nesigurnosti. Prikazani su eksperimentalni rezultati mjerenja poroznosti vulkanskih stijena. Kod mjerenja poroznosti dobivena je mjerna nesigurnost manja od 0,1 % u temperaturnom području od 10 do 30 °C.

Gljučne riječi: poroznost, vulkanska stijena, kapacitivno osjetljivi kristal, stohastička metoda

AUTHOR'S ADDRESS:

Assoc. Prof. Dr. Vojko Matko
University of Maribor
Faculty of Electrical Engineering and Computer Science
Smetanova 17, 2000 Maribor, SLOVENIA
phone: +386-02-220-7111
E-mail: vojko.matko@uni-mb.si

Received: 2003–11–14